Uncertainty Analysis of Interzonal Airflow Rates by Tracer Gas Methods

Hwataik Han and Seok-Hyo Cho
Kookmin University

ABSTRACT

Interzonal air movements are important to characterize overall ventilation performance of complicated multi-zone indoor spaces. Tracer gas techniques are widely used to measure ventilation rates or ventilation effectiveness as well as air movements between indoor spaces using either a single or multiple tracer gases. This paper compares the tracer gas methods in terms of procedures and uncertainties in measuring air exchange rates between rooms. Experiments have been conducted in a simple two-room model with known airflow rates. In a multi-gas experiment, the concentration decays of two tracer gases, i.e SF6 and R134a are measured after simultaneous injections in each room. A single tracer gas method is also applied by injecting SF6 gas with a time lag between two rooms. The data reduction procedures are developed to obtain the interzonal airflow rates using the matrix inversion method. Several data manipulation procedures are applied, which include data shift, interpolation, and smoothing of concentration data. Uncertainties of the calculated airflow rates are estimated depending on the intrinsic behavior of the airflow patterns and the data reduction procedures.

1. INTRODUCTION

In order to improve indoor air quality, the building code has been revised recently in Korea so that ventilation requirements have been specified for various types of buildings. In multi-zone buildings such as commercial or apartment buildings, the dilution rates and the source strengths are different from one zone to another. Even though the overall ventilation rates are satisfied by the code, the indoor environmental conditions can be different because of the interzonal airflows between zones. The airflows between zones can be either uni-directional or bi-directional. Even through the net airflow rate between zones is zero, there could be air exchanges by the equal amount. The estimation of interzonal airflow rate is important as much as the estimation of outdoor airflow rate in order to satisfy the ventilation requirements in multi-zone buildings.

Tracer gas experiments have been conducted to understand the transport of contaminants or to estimate the ventilation rates of buildings. Theoretical basis has been provided by Sinden (1978) for measuring interzonal and infiltration airflow rates in multi-zone environments. Sherman (1989) reviewed multi-tracer gas techniques and analyzed associated errors of using those techniques. Irwin (1990) conducted multi tracer gas experiments and compared the results with the analytical results by three different methods of numerical differentiation, numerical integration and eigenvalue approach. Nazaroff (1997) analyzed an eigenvalue problem with the nonlinear least-square method and compared with the results by multi-gas method. There have been attempts by Alfonso and Maldonando (1986) to measure interzonal airflows by single tracer gas methods.

In this paper, we conducted both single and multi tracer gas experiments in a two-zone experimental chamber and analyzed transient concentration data using various data processing methods. The results are compared with the

known interzonal airflow rates given in the chamber. Uncertainty analysis has been conducted to estimate the errors due to various data processing methods and the error sources associated with the parameters in obtaining interzonal airflow rates.

2. ANALYSIS

2.1 Model

The present two-zone model is shown schematically in Fig. 1. There are two rooms (A and B) and an exterior (E), and six airflow passages between these zones and the exterior.

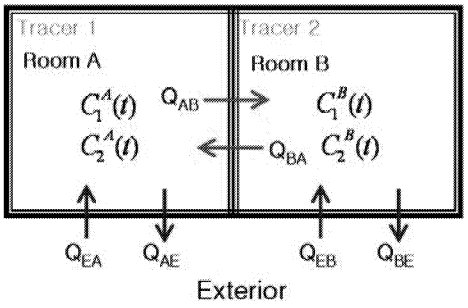

Figure 1: Two-zone model for interzonal air exchange experiment.

From the continuity equation in a stationary state for each room, the airflow rates should be in balance as follows.

$$Q_{AB} + Q_{AE} = Q_{BA} + Q_{EA} \quad (1a)$$

$$Q_{AB} + Q_{EB} = Q_{BA} + Q_{BE} \quad (1b)$$

The notation Q_{ij} means the airflow rate from zone "i" to zone "j". Hence, the Q_{ji} represents the airflow in the opposite direction through the same partition. The concentrations of tracer gas 1 and 2 in room A can be determined from unsteady mass balances in the room.

$$V_A \frac{d}{dt} C_1^A(t) = [C_E Q_{EA} + C_1^B Q_{BA} - C_1^A (Q_{AB} + Q_{AE})] \quad (2a)$$

$$V_A \frac{d}{dt} C_2^A(t) = [C_E Q_{EA} + C_2^B Q_{BA} - C_2^A (Q_{AB} + Q_{AE})] \quad (2b)$$

The superscript A represents room A, and the subscripts 1, 2 represent two different tracer gases. Similarly, the concentration changes in room B can be derived as follows.

$$V_B \frac{d}{dt} C_1^B(t) = [C_E Q_{EB} + C_1^A Q_{AB} - C_1^B (Q_{BA} + Q_{BE})] \quad (3a)$$

$$V_B \frac{d}{dt} C_2^B(t) = [C_E Q_{EA} + C_2^A Q_{AB} - C_2^B (Q_{BA} + Q_{BE})] \quad (3b)$$

2.2 Analytical Method

There are six equations and six unknowns of airflow rates. The above six equation can be expressed in a matrix form as in equation (4). The concentrations appear in the matrix [C] and the concentration changes appear in the right column. The equations have been rearranged in order, so that the diagonal elements have non zero or preferably large values. The inverse matrix of [C] has been obtained using the Gauss-Jordan elimination method.

$$\begin{vmatrix} -C_1^A & C_E & -C_1^A & C_1^B & 0 & 0 \\ 1 & -1 & 1 & -1 & 0 & 0 \\ 0 & 0 & C_1^A & -C_1^B & -C_1^B & C_E \\ -C_2^A & C_E & -C_2^A & C_2^B & 0 & 0 \\ 0 & 0 & C_2^A & -C_2^B & -C_2^B & C_E \\ 0 & 0 & 1 & -1 & -1 & 1 \end{vmatrix} \begin{vmatrix} Q_{AE} \\ Q_{EA} \\ Q_{AB} \\ Q_{BA} \\ Q_{BE} \\ Q_{EB} \end{vmatrix} = \begin{vmatrix} V_A \dot{C}_1^A \\ 0 \\ V_B \dot{C}_1^B \\ V_A \dot{C}_2^A \\ V_B \dot{C}_2^B \\ 0 \end{vmatrix} \quad (4)$$

3. EXPERIMENT

3.1 Experimental Setup

The overall experimental setup is shown in Fig. 2. It is composed of two rooms in the dimensions of 2 m x 2 m x 0.9 m. Mixing fans are installed in each room for complete mixing. There are six airflow control devices installed through the partitions between zones to generate known air exchange rates. Each airflow control device is composed of an air blower, a nozzle of 20 mm in diameter, and a damper in a 100 mm diameter duct. There are static pressure tabs across the nozzle to measure the airflow rate using a micro-manometer.

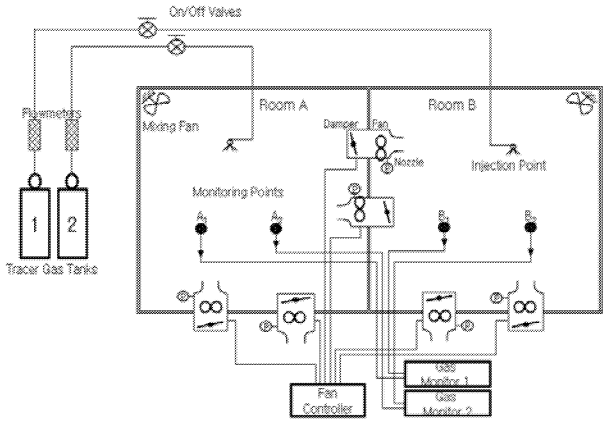

Figure 2: Schematic of the experimental setup.

Tracer gas tubes are connected from gas tanks to the rooms so that both tracer gases of SF6(Gas 1) and R134-a(Gas 2) can be injected into each room. The amounts of tracer gas injections are adjusted with flow meters and on/off valves by controlling the injection duration. The tube ends are located near mixing fans to ensure the injected gases to diffuse widely in each room. The concentrations of two tracer gases in both rooms are measured in sequence with a multi-sampler connected to a gas monitor. The lower limit of the gas monitor is reported to be 5ppm, and the accuracy is known to be about ± 5%. The sampling points are located in the middle of each room at the level of 1 m from the floor.

3.2 Experimental Method

Concentration decay methods are used in this study. In multi-tracer gas experiments, tracer gas 1 (SF6) is injected into room A, and tracer gas 2 (R134-a) is injected into room B simultaneously. In single tracer gas experiments, SF6 is injected into room A and B with a time delay. The initial concentrations are approximately in the order of 100 ppm. The data sampling interval is 1 minute. When the concentration becomes less than 1% of the initial value, data acquisition is stopped. Table 1 shows three different experimental conditions; leakage test (Run #0), interzonal airflow test (Run #1), and one-way airflow test (Run #2). Run #0 is an experiment to measure the air leakage of the room partitions with the fans not in operation. Run #1 has been conducted with all six fans in operation with balanced airflow rates, and Run #2 has been conducted with three fans in operation to create one-way airflow through the rooms.

Table 1: Experimental airflow conditions (CMH).

Run #	Description	Q_{AE}	Q_{EA}	Q_{AB}	Q_{BA}	Q_{BE}	Q_{EB}
0	Leakage	0	0	0	0	0	0
1	Interzone	6.2	4.2	3.9	5.9	3.8	5.8
2	One-way	0	4.0	4.0	0	4.0	0

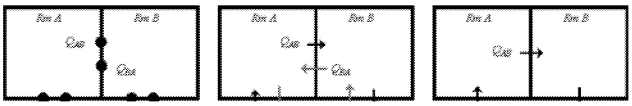

Figure 3. Schematics of the experimetal airflow conditions

4. RESULTS AND DISCUSSIONS

The concentration decays measured in the rooms are shown in Fig. 4 for Run #0. The leakage rates of the rooms are calculated to be less than 0.01 ACH. It is assumed to be relatively small compared to the air change rates of the other experiments which are in the order of 1-2 ACH.

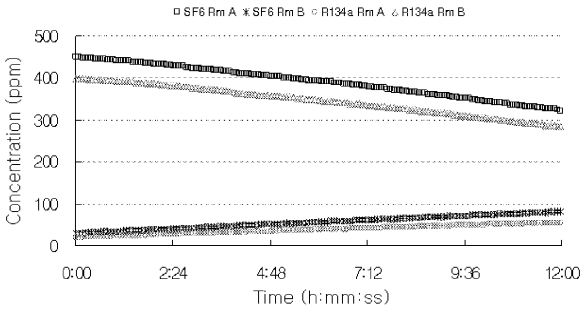

Figure 4: Decay concentration curves for Run #0.

The concentration variations for Run #1 are shown in Fig. 5 for both multi and single gas methods. The multi-gas results are shown above in the figure. The tracer gases injected in the rooms are observed to be transported into the adjacent rooms by air mixing between rooms with time delays. The concentrations in the

injection rooms decay monotonically with time. The concentrations in adjacent rooms, initially zero in concentration, increase to maximums and decay down afterwards. The single gas results show similar characteristics in one direction at a time. The graph looks as if two pairs of curves are displayed with a time delay.

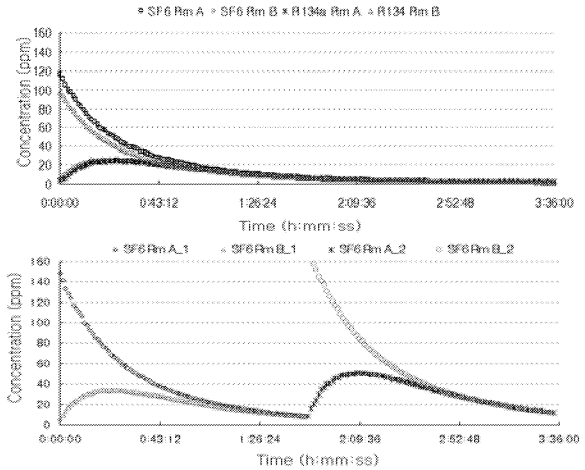

Figure 5: Decay concentration curves for Run #1

The results of Run #2 are shown in Fig. 6. Since the airflow is given in one direction; i.e. from the exterior to room A, B, and to the exterior sequentially, there would be negligible tracer movements in the opposite direction. It can be seen in the figure that the concentration in the upstream are very small.

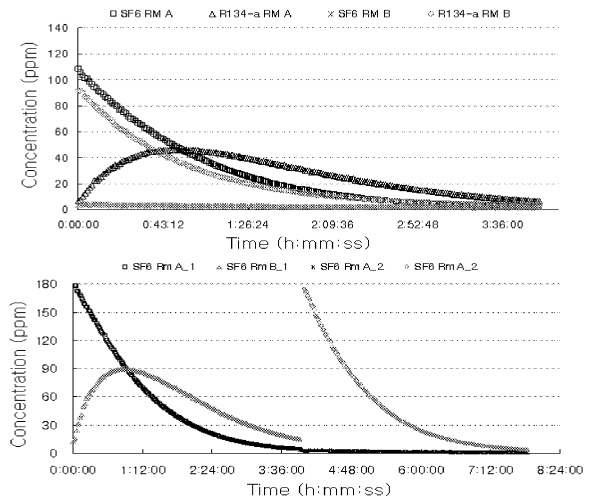

Figure 6: Decay concentration curves for Run #2.

In order to obtain airflow rates from the concentration data, the matrix equation are solved. As the concentrations and concentration slopes appearing in the matrix have their own uncertainties, these create uncertainties in estimating airflow rates. The raw data has been processed by shifting and smoothing in sequence. A data shift is necessary since the measurements are made alternately between rooms. The measurement in room B is delayed from that in room B by one sampling time of 30 seconds. Data smoothing has been conducted by averaging three data points in sequence. The data at the center is weighted twice compared to the neighboring data points (Han, 2007). The forward and the central differencing are also tested in calculating concentration slopes. Fig. 7 shows the results calculated according to the data processing methods. Three figures on the left hand side show the results by the forward differencing, and the right hand ones by the central differencing. The calculated results by raw data, shift data, and smoothed data are compared in the figure downwards. The scattering of the results are found to be considerably decreased by shifting and smoothing the raw data. The differencing methods, however, do not exhibit significant differences in results.

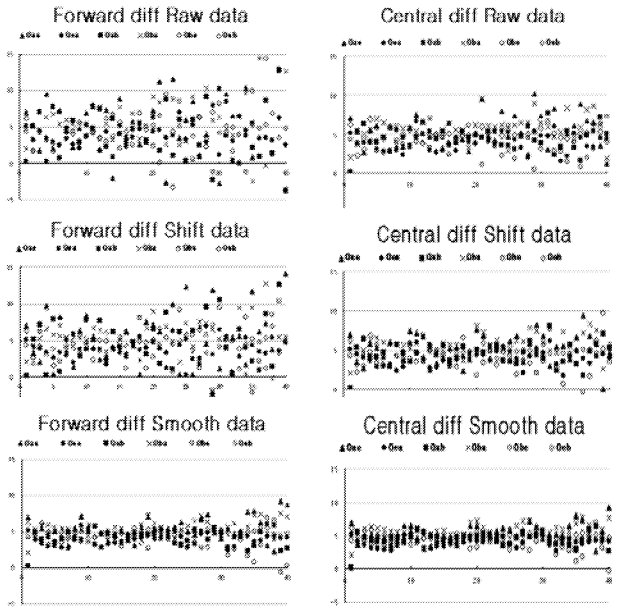

Figure 7: Distributions of the results depending on data manipulation procedures.

Even though the data processing helps in reducing the uncertainty, the uncertainty increases as time elapses. It is because the calculation is based on the concentration level as well as the concentration difference between the zones. The initial large concentration difference disappears between zones with time. It is hard to extrude meaningful results out of assimilated concentration distributions. In that sense, it is necessary to provide a criterion to cut off meaningless data after a certain period of time. In this paper, the expression (5) is used as a criterion for data cut-off, which uses the concentration slopes in the rooms and the difference in the concentration slopes.

$$\sqrt{\frac{(s_1^A)^2+(s_1^B)^2+(s_1^{A-B})^2}{3}} < \varepsilon \qquad (5)$$

$$\begin{aligned} s_1^A &= \dot{C}_1^A / \left(\dot{C}_1^A\right)_{t=0} \\ s_1^B &= \dot{C}_1^B / \left(\dot{C}_1^A\right)_{t=0} \\ s_1^{A-B} &= \left(\dot{C}_1^A - \dot{C}_1^B\right) / \left(\dot{C}_1^A\right)_{t=0} \end{aligned} \qquad (6)$$

where s_1^A and s_1^B are non-dimensional concentration slopes of tracer gas 1 in room A and B with respect to the initial maximum concentration, and s_1^{A-B} is the difference of the slopes. A similar criterion is applied to tracer gas 2, since the tracer gases are independent from each other. The value of ε has been chosen as 0.1 in the present experiments.

Table 2 shows the final results summarized according to the methods described so far. It shows the averages and standard deviations of airflow results. It also shows the errors of the six airflow rates compared to the given values. Quantitatively, the standard deviations are in the range of 1.6 CMH, and the relative errors are within 20%. The single gas method exhibits larger uncertainties compared to the multi-gas method.

In order to understand the major causes of uncertainties and the main factors affecting the results, the order of magnitude analysis has been conducted with some assumptions. The concentration in an adjacent room is assumed to be one order of magnitude smaller (δ<1) than that in an injection room. The concentration in each injection room is of the same order of magnitude. The relative error associated with a concentration slope is assumed to be greater compared to a concentration itself. In the present study, the airflow rate is greater in the direction from A to B, rather than B to A. These assumptions can be written as in equation (7), where $\dot{C}$ stands for a concentration slope, and ΔC stands for the uncertainty in C.

Table 2: Comparing the experimental results with the given airflow rates (CMH).

Run # (Multi-gas)		Q_{AE}	Q_{EA}	Q_{AB}	Q_{BA}	Q_{BE}	Q_{EB}
0	Average	0.07	0.07	0.04	0.05	0.08	0.08
	Std. deviation	0.03	0.03	0.02	0.01	0.05	0.05
1	Average	5.37	3.95	4.44	5.86	3.46	4.89
	Std. deviation	1.51	0.60	1.06	1.28	1.33	0.42
	Error	13%	6%	15%	1%	5%	17%
2	Average	0.20	3.59	4.03	0.24	3.92	0.13
	Std. deviation	1.45	0.46	1.02	0.25	0.85	0.93
	Error	-	10%	3%	-	1%	-

Run # (Single-gas)		Q_{AE}	Q_{EA}	Q_{AB}	Q_{BA}	Q_{BE}	Q_{EB}
1	Average	4.98	3.82	4.67	5.84	3.21	4.38
	Std. deviation	1.66	0.75	0.96	1.34	1.58	0.69
	Error	19%	10%	18%	2%	12%	25%
2	Average	-0.72	3.10	3.86	0.04	3.59	-0.23
	Std. deviation	1.20	0.46	1.02	0.02	0.82	0.77
	Error	-	21%	2%	-	9%	-

$$\begin{aligned} &\frac{O(C_1^B)}{O(C_1^A)} \approx \frac{O(C_2^A)}{O(C_2^B)} \approx \delta \\ &O\left(\frac{\Delta C}{C}\right) < O\left(\frac{\Delta \dot{C}}{\dot{C}}\right) \\ &O\left(\frac{\Delta \dot{C}_1^A}{\dot{C}_1^A}\right) \approx O\left(\frac{\Delta \dot{C}_2^B}{\dot{C}_2^B}\right) < O\left(\frac{\Delta \dot{C}_2^A}{\dot{C}_2^A}\right) \approx O\left(\frac{\Delta \dot{C}_1^B}{\dot{C}_1^B}\right) \end{aligned} \qquad (7)$$

The expected highest error of each airflow rate is derived based on the sum of the least squares of errors from the inverse of the matrix (4). The uncertainties of Q_{EB}, Q_{AB}, Q_{AE} are found to be greater than the rest of three airflow rates intrinsically. The relative magnitudes of errors are compared each other in equation (8). This fact is confirmed from the magnitudes of errors shown in Table 2.

$$\left.\frac{\Delta Q}{Q}\right|_{AB} \approx \left.\frac{\Delta Q}{Q}\right|_{AE} \approx \left.\frac{\Delta Q}{Q}\right|_{EB} > \left.\frac{\Delta Q}{Q}\right|_{BA} \approx \left.\frac{\Delta Q}{Q}\right|_{BE} \approx \left.\frac{\Delta Q}{Q}\right|_{EA} \quad (8)$$

5. CONCLUSION

In this paper, uncertainty analysis has been conducted for interzonal airflow rates using single and multi tracer gas methods. Uncertainties are estimated according to data processing methods and the orders of magnitudes are derived by the parametric considerations of the uncertainties.

- The interzonal airflow rates are present even though the net ventilation rate is zero, and can be measured by multi-gas or repeated single gas methods.
- The error ranges can be considerably reduced by processing concentration data in various ways. It is desirable to synchronize concentration data between zones by shifting a set of data in one zone and to smooth data by averaging before estimating concentration slopes.
- As the initial tracer concentration decays, the concentrations between zones become not distinguishable as time passes. The data cut-off helps to reduce overall uncertainties by excluding assimilated data afterwards. The concentration slopes and the root mean square values of the slopes are suggested to be less than 10% of the maximum initial concentration slope.
- The uncertainty analysis indicates that the concentration slope in an adjacent room affects the uncertainties of the airflow rates most. The orders of magnitudes of the uncertainties are in good agreements qualitatively with the uncertainties obtained experimentally.

Further researches are required to reduce uncertainties associated with tracer gas experimental methods to measure interzonal airflow rates.

ACKNOLWLEDGEMENTS

This research was supported by a grant (06ConstructionCoreB02) from Construction Core Technology Program by Ministry of Construction & Transportation of Korean government.

REFERENCES

Afonso, C. & Maldonando, E. (1986), A Single Tracer-gas Method to Characterize Multi-room Air Exchanges, Energy and Buildings, Vol. 9, pp. 273-280.

Han, H. (2003), Mechanical Measurement, pp. 43-45.

Han, H. (2007), An Experiment on Verification of Multi-Gas Tracer Technique for Air Exchange Rate Between Rooms, Proc. of the SAREK 2007 Winter Annual Conference, pp. 99-104.

Irwin, C. & Edwards, R. (1990), A Comparison of Different Methods of Calculating Interzonal Airflows by Multiple Tracer Gas Decay Tests, Progress and Trends in Air Infiltration and Ventilation Research, Proc. of 10th AIVC Conf., IEA, Finland, Vol. 1, pp. 57-70.

Nazaroff, W. (1997), Nonlinear Least- squares Minimization Applied to Tracer Gas Decay for Determining Airflow Rates in a Two-zone Building, Indoor Air, Vol. 7, pp. 64-75.

Sherman, M. (1989), On the Estimation of Multizone Ventilation Rates from Tracer Gas Measurements, Building and Environments, Vol. 24, pp. 355-362.

Sinden, F. (1978), Multi-chamber Theory of Air Infiltration, Building and Environment, Vol. 13, pp. 21-28.